International Journal of Solids and Structures 46 (2009) 2539–2546

Contents lists available at ScienceDirect

International Journal of Solids and Structures

journal homepage: www.elsevier.com/locate/ijsolstr

Hybrid theoretical, experimental and numerical study of vibration and buckling of composite shells with scatter in elastic moduli

Xiaojun Wang [a,*], Isaac Elishakoff [b], Zhiping Qiu [a], Changhe Kou [a]

[a] Institute of Solid Mechanics, Beijing University of Aeronautics and Astronautics, No.37 Xueyuan Road, Haidian District, Beijing 100083, China
[b] Department of Mechanical Engineering, Florida Atlantic University, Boca Raton FL 33431-0991, USA

ARTICLE INFO

Article history:
Received 2 August 2008
Received in revised form 11 December 2008
Available online 29 January 2009

Keywords:
Hybrid theoretical
Experimental and numerical method
Ellipsoidal analysis
Interval analysis
Experimental data
Composite shell

ABSTRACT

Hybrid theoretical, experimental and numerical method is proposed for free vibration and buckling of composite shell with unavoidable scatter in elastic moduli. Based on the Goggin's measurement techniques, the elastic moduli for material T300-QY8911 are measured, and a set of experimental points are obtained. The measurements of elastic moduli are quantified by either (1) the smallest ellipsoid and (2) the smallest four-dimensional uncertainty hyper-rectangle. Then uncertainty propagation in vibration and buckling problems of composite shell by ellipsoidal analysis and interval analysis are, respectively, studied from the theoretical standpoint. Comparison between these analyses is performed numerically.

1. Introduction

Due to high strength-to-weight and stiffness-to-weight ratios, composite materials are widely used in various types of engineering structures. However, usually composite materials experience larger uncertainties in their material properties than conventional materials due to a number of parameters involved in their fabrication and manufacturing processes (Tewary, 1978). In past years, extensive literatures were devoted to study the influence of the uncertainties on the mechanical performance of the composite structures, including probabilistic method and non-probabilistic method. For example, Ramu and Ganesan (1993) treated the scatter in material properties within the realm of stochastic finite element method. When the available limited uncertain information is not sufficient to determine the probabilistic characteristics of uncertain parameters, the non-probabilistic methods were shown to possess great advantage. Elishakoff, Li and Starnes used convex modeling to incorporate uncertainties in elastic moduli into the structural analysis (Elishakoff et al., 2001). Qui (2005) performed a comparison between convex models and interval analysis method to predict the effect of uncertain-but-bounded parameters on the buckling of composite structures. Nevertheless, these studies evaluated only the bounds of natural frequency or buckling load based on the presumed hyper-rectangular or ellipsoidal uncertainties. The basic precondition, namely the problem of where these hyper-rectangle or ellipsoid of uncertainty were coming from, was not addressed. This resulted in the difficulty of applications of both convex models and interval analysis in practical problems. Pantelides adopted convex models to examine the buckling and postbuckling behaviour of thin-walled stiffened elements under uniform compression with geometric and material uncertainties (Pantelides, 1996). Based on Goggin's experimental data (Goggin, 1973), variations of natural frequency and buckling load due to uncertainty in material properties by convex modeling were predicted by Li et al. (1996). In the paper by Wang et al. (2008), two methods for uncertainty quantification, namely, convex modeling and interval analysis, were extensively compared by use of the simulated data points, where the smallest ellipsoid and the smallest hyper-rectangle enclosing them were determined.

The present paper proposes a *hybrid theoretical, experimental and numerical method* to investigate uncertainties in the elastic moduli. It gives a complete procedure of uncertainty analysis, containing three parts. The first part is to quantify the uncertainty based on the real experimental data points. The second part constitutes the theoretical analysis of the uncertainty propagation in the structural problems at hand. The third part is represented by numerical investigation. The procedures outlined in this paper are deemed to provide a needed tool not just for an intellectual exercise, but for solution of the practical problems involving uncertainty.

2. Problem statement

Cylindrical shells of composite materials are usually significant parts of the engineering structures. Free vibration and buckling of

* Corresponding author.
E-mail addresses: xjwang@buaa.edu.cn (X. Wang), elishako@fau.edu (I. Elishakoff), zpqiu@buaa.edu.cn (Z. Qiu).

0020-7683/$ - see front matter © 2009 Elsevier Ltd. All rights reserved.
doi:10.1016/j.ijsolstr.2009.01.018

composite cylindrical shell with simply supported boundary conditions have been extensively studied in previous literature.

The closed-form expressions for the natural frequency and the buckling load (for details see Appendix), are, respectively,

$$\omega_{mn,0}^2 = \frac{1}{\rho}\left[C_{33} + \frac{(2C_{12}C_{23} - C_{13}C_{22})C_{13} - C_{23}^2 C_{11}}{C_{11}C_{22} - C_{12}^2}\right] \tag{1}$$

and

$$p = \frac{2}{(\lambda_m^2 + 2\lambda_n^2)R}\left[C_{33} + \frac{(2C_{12}C_{23} - C_{13}C_{22})C_{13} - C_{23}^2 C_{11}}{C_{11}C_{22} - C_{12}^2}\right] \equiv p_{mn} \tag{2}$$

From Eqs. (1) and (2), it can be seen that before any prediction can be made on the vibration and buckling properties of the composite shell, the values of the elastic moduli should be known in advance. However, due to the scatter or uncertainty in elastic moduli stemming from their fabrication and manufacturing processes, the influences of them on the natural frequency and buckling load need to be analyzed.

In the following, based on the real experimental data points obtained by one of us (C.K.), ellipsoidal and interval analyses will be adopted to quantify uncertainties of the elastic moduli and investigate their propagation in the free vibration and buckling of the composite cylindrical shell.

3. Ellipsoidal and interval analyses

3.1. Convex modeling and interval modeling of experimental data for elastic moduli of T300-QY8911

Before the analysis of uncertainty propagation, the uncertain elastic moduli need to be quantified. By virtue of the concept in the paper by Wang et al. (2008), we will determine the smallest ellipsoid and the smallest hyper-rectangular containing the real experimental data of the elastic moduli for T300-QY8911.

The elastic modulus in the first direction E_1, the elastic modulus in the second direction E_2, the Poisson ratio υ_{21} and the shear modulus G_{12} are measured. The four parameters constitute a four-dimensional parameter space, namely, $E = (E_1, E_2, \upsilon_{21}, G_{12})^T$. Experimental techniques given by Goggin (1973) and adopted by Elishakoff et al. (2001) are used to measure these elastic moduli. Table 1 shows the measured 18 data points of the elastic moduli for T300-QY8911.

The 18 experimental points are represented by $E^{(r)}(r = 1,2,\ldots,18)$. By the method introduced in the paper by Wang et al. (2008), convex modeling assumes that all these experimental points belong to an ellipsoid

$$Z(W,\theta) = \{E : E \in R^4,\ (E - E_0)^T W (E - E_0) \leqslant 1\} \tag{3}$$

where E_0 is the state vector of the central point of the ellipsoid, and W is the weight matrix. Interval modeling assumes that all experimental points belong to a hyper-rectangle.

By using transformation matrix $T_N(\theta_1, \theta_2, \ldots, \theta_{N-1})$ given in the paper (Zhu et al., 1996), the above 18 points in the rotated coordinate system will have their new coordinates denoted by $b^{(r)}(r = 1,2,\ldots,18)$. Here, $N = 4$, so the transformation matrix will be

$$T_4(\theta_1,\theta_2,\theta_3) = \begin{bmatrix} \cos\theta_1 & -\sin\theta_1 & 0 & 0 \\ \sin\theta_1\cos\theta_2 & \cos\theta_1\cos\theta_2 & -\sin\theta_2 & 0 \\ \sin\theta_1\sin\theta_2\cos\theta_3 & \cos\theta_1\sin\theta_2\cos\theta_3 & \cos\theta_2\cos\theta_3 & -\sin\theta_3 \\ \sin\theta_1\sin\theta_2\sin\theta_3 & \cos\theta_1\sin\theta_2\sin\theta_3 & \cos\theta_2\sin\theta_3 & \cos\theta_3 \end{bmatrix} \tag{4}$$

To obtain the smallest ellipsoid, let us first examine a four-dimensional box of the form

$$|b - b_0| \leqslant d \tag{5}$$

which contains all 18 points. The vector of semi-axes $d = (d_1, d_2, d_3, d_4)^T$ and the vector of central points $b_0 = (b_{10}, b_{20}, b_{30}, b_{40})^T$ of the "box" in the rotated coordinate system are given by

$$\begin{aligned} d_k &= \tfrac{1}{2}\left(\max_r\left(b_k^{(r)}\right) - \min_r\left(b_k^{(r)}\right)\right), \\ b_{k0} &= \tfrac{1}{2}\left(\max_r\left(b_k^{(r)}\right) + \min_r\left(b_k^{(r)}\right)\right), \end{aligned} \quad (r = 1,2,\ldots,18;\ k = 1,2,3,4) \tag{6}$$

We now enclose this box by an ellipsoid

$$\sum_{k=1}^{4}\frac{(b_k - b_{k0})^2}{g_k^2} \leqslant 1 \tag{7}$$

where g_k are the semi-axes of the ellipsoid. There are infinite number of ellipsoids which contain the box given in Eq. (5). Clearly, the best choice is the one with minimum volume. The volume of an m-dimensional ellipsoid is given by

$$V_e = C_4\prod_{k=1}^{4} g_k \tag{8}$$

where C_4 is a constant.

Following the monograph by Elishakoff et al. (2001) and the paper by Qiu (2003), the semi-axes of the smallest ellipsoid should be

$$g_i = \sqrt{m}d_i \quad (i = 1,2,3,4) \tag{9}$$

Thus, once the size of the box Eq. (5) is known, the semi-axes of the minimum-volume ellipsoid enclosing the box of the experimental data are readily determined by utilizing Eq. (9). If there are no experimental points at the corner of the box, the size of such an ellipsoid may further be reduced until one of the experimental points reaches the surface of the ellipsoid. The semi-axes of the ellipsoid in this case may be replaced by ηg_k, where the factor is determined from the condition

$$\eta = \sqrt{\max_r \sum_{k=1}^{4}\frac{\left(b_k^{(r)} - b_{k0}\right)^2}{g_k^2}} \leqslant 1, \quad (r = 1,2,\ldots,18) \tag{10}$$

If there are some experimental points in the corner of the multi-dimensional box, the factor η equals unity. The ellipsoid (7) can be written in the form

$$(b - b_0)^T D (b - b_0) \leqslant 1 \tag{11}$$

Table 1
Experimental data of the elastic moduli for T300-QY8911.

No.	E_1 (GPa)	E_2 (GPa)	υ_{21}	G_{12} (GPa)
1	129.20	9.34	0.28	5.23
2	131.59	9.53	0.33	4.97
3	130.63	9.08	0.33	5.16
4	132.01	9.34	0.33	5.15
5	131.04	8.94	0.34	5.15
6	120.61	9.04	0.33	4.81
7	127.69	8.99	0.32	5.11
8	133.65	9.36	0.35	5.08
9	132.19	9.07	0.30	4.85
10	132.00	9.73	0.35	5.00
11	130.39	9.21	0.34	5.34
12	128.28	8.67	0.33	4.98
13	135.30	9.18	0.32	5.13
14	137.33	9.28	0.33	5.25
15	141.69	10.73	0.31	5.47
16	126.91	9.39	0.33	5.65
17	133.75	9.34	0.32	5.33
18	129.24	9.35	0.32	5.16

in which b_0 is the vector of central points whose components are given by Eq. (6), and D is a diagonal matrix

$$D = diag\left((\eta g_1)^{-2}, (\eta g_2)^{-2}, (\eta g_3)^{-2}, (\eta g_4)^{-2}\right) \tag{12}$$

The volume of the ellipsoid now reads

$$V_e = C_4 \eta^4 \prod_{k=1}^{4} g_k \tag{13}$$

which is a function of a set of parameters $\theta_k (k = 1,2,3)$. Therefore, the best ellipsoid among these ellipsoids is the one which contains all given points and possesses the minimum volume, i.e.,

$$V_e = \min_{\theta_1,\theta_2,\theta_3} \{V_e(\theta_1, \theta_2, \theta_3)\} \tag{14}$$

A possible approach to determine this ellipsoid is to search among all possible cases by increasing $\theta_k (k = 1,2,3)$ from 0 to $\pi/2$ in sufficiently small increments $\Delta\theta_k$, and to compare the volumes of so obtained ellipsoids. Once one finds the ellipsoid with minimum volume in one direction, say $\theta_{k0} (k = 1,2,3)$, the ellipsoid can be transformed back into the original coordinate system by applying the transformation matrix T_4. Hence, the vector a_0 of central point and the weight matrix W in Eq. (3) become

$$E_0 = T_4^T b_0, \quad W = T_4^T D T_4 \tag{15}$$

where $T_4 = T_4(\theta_{10}, \theta_{20}, \theta_{30})$. So Eq. (15) constitutes the smallest ellipsoid containing all experimental points. The "box" corresponding to the smallest ellipsoid is the smallest hyper-rectangle.

In order to avoid the numerical problem due to the different order of magnitude for elastic moduli, the dimensionless uncertainty coefficients of elastic moduli are introduced as follows:

$$e_1 = \frac{E_1}{131.0\ (\mathrm{GPa})},\ e_2 = \frac{E_2}{9.4\ (\mathrm{GPa})},\ \mu_{21} = \frac{\nu_{21}}{0.3},\ g_{12} = \frac{G_{12}}{5.3\ (\mathrm{GPa})} \tag{16}$$

So the data points for the uncertainty coefficients of elastic moduli can be obtained as Table 2.

According to the experimental data shown in Table 2, the optimal rotation angle is $\theta^* = (\theta_{10}, \theta_{20}, \theta_{30}) = (38°, 30°, 60°)$, which implies that the smallest ellipsoid is not parallel to the global coordinate system, and the dimensionless e_0 and W can be obtained as

$$e_0 = (e_1, e_2, \mu_{21}, g_{12})^T = (1.0189, 1.0185, 1.0405, 0.9652)^T \tag{17}$$

and

$$W = \begin{bmatrix} 148.2163 & -89.0543 & 7.9058 & -2.3375 \\ -89.0543 & 103.8088 & 10.1189 & -2.9919 \\ 7.9058 & 10.1189 & 49.0595 & -6.5762 \\ -2.3375 & -2.9919 & -6.5762 & 65.2416 \end{bmatrix} \tag{18}$$

Corresponding to the smallest ellipsoid, the smallest hyper-rectangle also can be obtained. Its 16 vertices are given in Table 3, which can be denoted by the following set

$$\hat{e} = \{e : e \in R^4, e = e^{(i)}, i = 1, 2, \ldots, 16\} \tag{19}$$

It can be seen from Table 3 that the smallest hyper-rectangular is also not parallel to the global coordinate system.

3.2. Determination of bounds on the natural frequency and buckling load

After quantifying the elastic moduli with the ellipsoid and the hyper-rectangle based the measured experimental points, both ellipsoidal and interval analyses for uncertainty propagation in the free vibration and buckling problems ought be proceeded. As has been stated in the previous section, the objective function (the natural frequency $\omega_{mn,0}$ or the critical external pressure p_{mn}) of the composite shell depends on the four basic elastic moduli. One can also discuss the natural frequency $\omega_{mn,N}$ if the external pressure is present, having in mind that the external pressure is below its critical value. For the sake of generality, in the following analysis, a generic formula for the objective function is adopted instead of relying on a more concrete expression such as Eq. (1) or (2).

The objective function is written in the following generic form:

$$F = F(e_1, e_2, \mu_{21}, g_{12}),\ F = \omega_{mn,0} \text{ or } p_{mn} \tag{20}$$

or more simply

$$F = F(e_i),\ (i = 1, 2, 3, 4) \tag{21}$$

where $e_3 = \nu_{21}$ and $e_4 = g_{12}$. The function F in the above equation also depends on the form of structure, boundary conditions as well as geometric properties.

Let $e_i^0 (i = 1, 2, 3, 4)$ be the nominal values of the elastic moduli, which can be derived from Eq. (17). Then, the elastic moduli of values different from those nominal values could be denoted as $e_i^0 + \delta_i$, δ_i being deviations from nominal values. So the deviation vector will be $\delta^T = (e - e_0)^T = (\delta_1, \delta_2, \delta_3, \delta_4)$. The objective function corresponding to these elastic moduli, retaining only the first order terms in δ_i, is written as follows:

$$F(e_i^0 + \delta_i) = F(e_i^0) + f^T \delta \tag{22}$$

Table 2
The dimensionless uncertainty coefficients of the elastic moduli for T300-QY8911.

No.	e_1	e_2	μ_{21}	g_{12}
1	0.9863	0.9936	0.9333	0.9868
2	1.0045	1.0138	1.1000	0.9377
3	0.9972	0.9660	1.1000	0.9736
4	1.0077	0.9936	1.1000	0.9717
5	1.0003	0.9511	1.1333	0.9717
6	0.9207	0.9617	1.1000	0.9075
7	0.9747	0.9564	1.0667	0.9642
8	1.0202	0.9957	1.1667	0.9585
9	1.0091	0.9649	1.0000	0.9151
10	1.0076	1.0351	1.1667	0.9434
11	0.9953	0.9798	1.1333	1.0075
12	0.9792	0.9223	1.1000	0.9396
13	1.0328	0.9766	1.0667	0.9679
14	1.0483	0.9872	1.1000	0.9906
15	1.0816	1.1415	1.0333	1.0321
16	0.9688	0.9989	1.1000	1.0660
17	1.0210	0.9936	1.0667	1.0057
18	0.9866	0.9947	1.0667	0.9736

Table 3
Vertices of the smallest hyper-rectangle.

No.	$(e_1, e_2, \mu_{21}, g_{12})$
$e^{(1)}$	(0.8863, 0.9177, 1.0034, 0.9868)
$e^{(2)}$	(0.9326, 0.9769, 1.1335, 1.0736)
$e^{(3)}$	(0.9094, 0.9473, 1.0684, 0.8568)
$e^{(4)}$	(0.9557, 1.0065, 1.1985, 0.9436)
$e^{(5)}$	(1.0153, 1.0828, 0.8825, 0.9868)
$e^{(6)}$	(1.0615, 1.1420, 1.0126, 1.0736)
$e^{(7)}$	(1.0384, 1.1123, 0.9474, 0.8568)
$e^{(8)}$	(1.0846, 1.1715, 1.0776, 0.9436)
$e^{(9)}$	(0.9532, 0.8655, 1.0034, 0.9868)
$e^{(10)}$	(0.9995, 0.9247, 1.1335, 1.0736)
$e^{(11)}$	(0.9763, 0.8951, 1.0684, 0.8568)
$e^{(12)}$	(1.0226, 0.9543, 1.1985, 0.9436)
$e^{(13)}$	(1.0821, 1.0305, 0.8825, 0.9868)
$e^{(14)}$	(1.1284, 1.0897, 1.0126, 1.0736)
$e^{(15)}$	(1.1052, 1.0601, 0.9474, 0.8568)
$e^{(16)}$	(1.1515, 1.1193, 1.0776, 0.9436)

where

$$f^T = \left(\frac{\partial F(e_i^0)}{\partial e_1}, \frac{\partial F(e_i^0)}{\partial e_2}, \frac{\partial F(e_i^0)}{\partial e_3}, \frac{\partial F(e_i^0)}{\partial e_4}\right) \tag{23}$$

Based on the smallest ellipsoid (3), the deviation δ from the nominal elastic moduli is to vary in the following ellipsoidal set

$$Z(W,\theta) = \{\delta : \delta \in R^4, \delta^T W \delta \leqslant \theta^2\} \tag{24}$$

where the size parameter θ is set equal to unity and the weight matrix W can be obtained from Eq. (18).

If *ellipsoidal analysis* (Chernousko, 1993) is adopted, then the problem is formulated as follows: based on the ellipsoid (24) of the elastic moduli, find the extreme natural frequency (or the critical external pressure)

$$F_{ext} = \underset{\delta \in Z(W,\theta)}{extermum} \left(F(e_i^0) + f^T \delta\right) \tag{25}$$

In Eq. (25), F_{ext} is the lowest or the highest value of the fundamental natural frequency (or the critical external pressure) of the composite structure with the elastic moduli varying within the range of the ellipsoidal set Z. Since Eq. (25) calls for finding the extremum of the linear functional $f^T\delta$ on the convex set $Z(W,\theta)$, the extreme values take place on the set of the extreme points, or the boundary, of the set Z as discussed by Ben-Haim and Elishakoff (1990) and Qui (2005).

To arrive at the extreme values, we use the method of Lagrange multipliers. Since the analysis which follows is mathematically analogous to that described in monograph by Ben-Haim and Elishakoff (1990), here we only list the final result. The extreme values of the objective function F result in the following expressions:

$$\begin{aligned} \omega_{mn,\max} &= \langle \omega_{mn,0} \rangle + \theta \sqrt{f_\omega^T W^{-1} f_\omega}, \\ \omega_{mn,\min} &= \langle \omega_{mn,0} \rangle - \theta \sqrt{f_\omega^T W^{-1} f_\omega} \\ p_{cr,\max} &= \langle p_{cr} \rangle + \theta \sqrt{f_p^T W^{-1} f_p}, \\ p_{cr,\min} &= \langle p_{cr} \rangle - \theta \sqrt{f_p^T W^{-1} f_p} \end{aligned} \tag{26}$$

where $\langle \omega_{mn,0} \rangle = \omega_{mn,0}(e_1^0, e_2^0, e_3^0, e_4^0)$ and $\langle p_{cr} \rangle = p_{cr}(e_1^0, e_2^0, e_3^0, e_4^0)$ are values of the natural frequency and critical extreme pressure calculated at the middle values of the elastic moduli, and

$$f_\omega^T = \left(\frac{\partial \omega_{mn,0}(e_i^0)}{\partial e_1}, \frac{\partial \omega_{mn,0}(e_i^0)}{\partial e_2}, \frac{\partial \omega_{mn,0}(e_i^0)}{\partial e_3}, \frac{\partial \omega_{mn,0}(e_i^0)}{\partial e_4}\right) \tag{27}$$

$$f_p^T = \left(\frac{\partial p_{cr}(e_i^0)}{\partial e_1}, \frac{\partial p_{cr}(e_i^0)}{\partial e_2}, \frac{\partial p_{cr}(e_i^0)}{\partial e_3}, \frac{\partial p_{cr}(e_i^0)}{\partial e_4}\right) \tag{28}$$

If *interval analysis* (Moore, 1979; Alefeld and Herzberger, 1983; Neumaier, 1990; Hansen, 1992) is adopted, then the problem is formulated as follows: based on the hyper-rectangle of the elastic moduli from Table 3, find the extreme natural frequency (or the critical external pressure). Due to the convexity of the derived smallest hyper-rectangle and the linearity of Eq. (22), the extreme values of the objective function F will reach at the 16 vertices in Table 3, i.e.,

$$\omega_{mn} = \min\{\omega_{mn}^{(i)},\ i = 1,2,\ldots,16\}, \quad \bar{\omega}_{mn} = \max\{\omega_{mn}^{(i)},\ i = 1,2,\ldots,16\} \tag{29}$$

and

$$p_{cr} = \min\{p_{cr}^{(i)},\ i = 1,2,\ldots,16\}, \quad \bar{p}_{cr} = \max\{p_{cr}^{(i)},\ i = 1,2,\ldots,16\} \tag{30}$$

where $\omega_{mn}^{(i)} = \omega_{mn}(e^{(i)})$ and $p_{cr}^{(i)} = p_{cr}(e^{(i)})(E^{(i)} = (e_1^{(i)}, e_2^{(i)}, e_3^{(i)}, e_4^{(i)}))$ are values of the natural frequency and critical extreme pressure calculated at the vertices of the elastic moduli.

From the above ellipsoidal and interval analyses, the upper- and lower-bounds of the natural frequency ω and the critical external pressure p_{cr}, respectively, can be calculated by using the approximate expression for F. These results show that the uncertainties in elastic moduli have a significant effect on the values of the natural frequency and the buckling load of the composite structure.

4. Numerical examples

In order to illustrate the efficacy the presented hybrid method, numerical analysis of two cases of the free vibration and buckling problems of composite shells will be used to investigate the influence of uncertainties in the material properties for T300-QY8911 on the natural frequency and buckling load.

The derived smallest ellipsoid Eqs. (17) and (18) and the vertices of the derived smallest hyper-rectangular in Table 3 obtained from the experimental data in Table 1 are used in the following ellipsoidal analysis (EA) and interval analysis (IA), respectively.

Consider the composite cylindrical shell with a radius R = 125.0 mm and the thickness of each laminate t = 0.5 mm subject to simply supported boundary conditions. The length of the shell is L = 2000.0 mm. The density of T300-QY8911 is 1380.0 kg/m^3. The following two cases are considered:

Case 1: The 10-layer laminated shell, with ply angle being $[\theta, -\theta, \theta, -\theta, \theta]_{sym}$, θ ranging from 0° to 90°.

Case 2: The 5-layer laminated shell, with ply angle being $[\theta, -\theta, \theta, -\theta, \theta]$, θ ranging from 0° to 90°.

The percentage value β is defined to quantify the degree of uncertainty of the natural frequency or the critical external pressure of the composite shell as follows:

$$\beta = (F_u - F)_l / 2F_n \times 100\% \tag{31}$$

where subscripts u, l and n, respectively, denote the upper-bound, lower-bound and the nominal value.

The variability of the fundamental natural frequency and the critical external pressure obtained by ellipsoidal and interval analyses are shown in Figs. 1 and 2 for the 10-layer laminated cylindrical shell, and Figs. 3 and 4 for the 5-layer laminated cylindrical shell, where the abrupt turns at some points of these curves imply the change of vibration or buckling mode. Figs. 5–8 portray the percentagewise degree of uncertainty of the fundamental natural frequency and the critical external pressure corresponding to Figs. 1–4, respectively.

It can be seen from these figures that the effect of uncertainty in elastic moduli on both the fundamental natural frequency and the critical external pressure varies greatly with the laminate configuration and the number of layers of the composite shell. It is remarkable that the variability of the critical external pressure due to the uncertainty in elastic moduli is bigger than that of the fundamental natural frequency. For example, the percentagewise degree of uncertainty for the fundamental natural frequency is about 5%, while that for the critical external pressure is about 11%. From Figs. 5–8, it appears that certain differences exist between the degree of uncertainty predicted by ellipsoidal analysis and interval analysis. In fact, numerically the maximum differences between the two methods only are 0.53%, 1.66%, 0.85% and 3.1% for the four results given in Figs. 5–8. Therefore, both ellipsoidal modeling and interval analysis appear to constitute viable methods for uncertainty quantification.

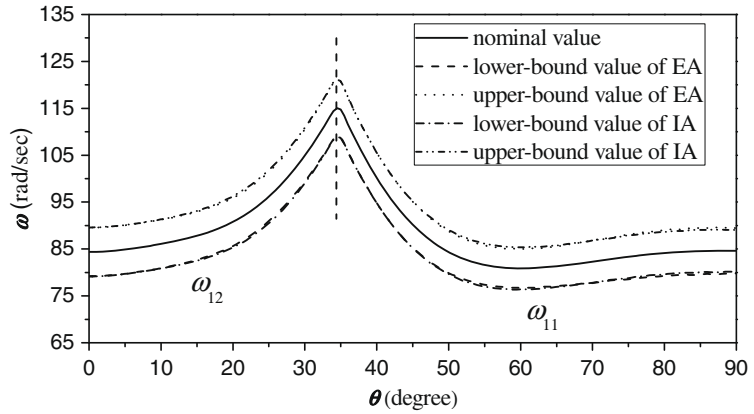

Fig. 1. Variability of the fundamental natural frequency for the 10-layer laminated cylindrical shell.

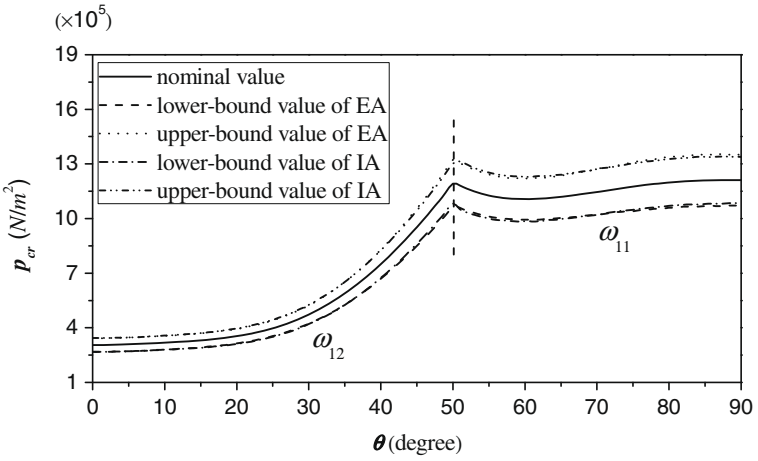

Fig. 2. Variability of the critical external pressure for the 10-layer laminated cylindrical shell.

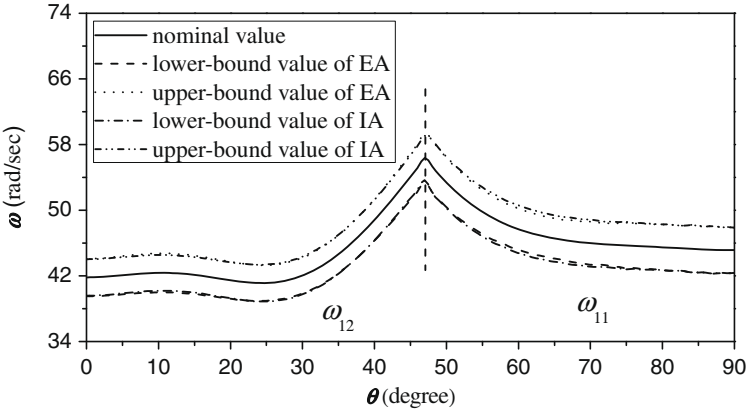

Fig. 3. Variability of the fundamental natural frequency for the 5-layer laminated cylindrical shell.

5. Conclusion

In this paper, a hybrid theoretical, experimental and numerical method is proposed to evaluate the influence of the scatter in elastic moduli on the natural frequency and critical external pressure of composite shell. The smallest ellipsoid and hyper-rectangle containing the measured experimental points for material T300-QY8911 are derived, which may be not parallel to the global coordinate system. Based on the obtained ellipsoid and hyper-rectangle, uncertainty propagation in vibration and buckling problems are studied by ellipsoidal analysis and interval analysis. The results of theoretical analysis and numerical analysis show that there is a significant influence of scatter in elastic moduli on both the natural frequency and critical buckling load of composite shell.

This study proposes a complete framework for uncertainty analysis in structures with uncertain parameters. Remarkably, it makes both ellipsoidal modeling and interval analysis as practical tools apparently for the first time in the literature.

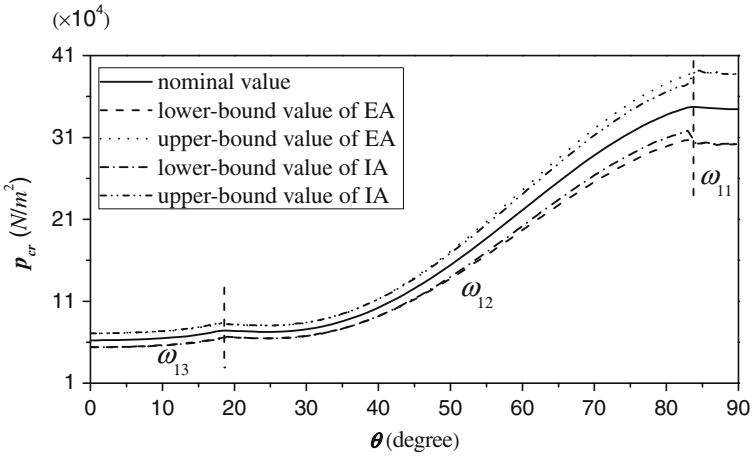

Fig. 4. Variability of the critical external pressure for the 5-layer laminated cylindrical shell.

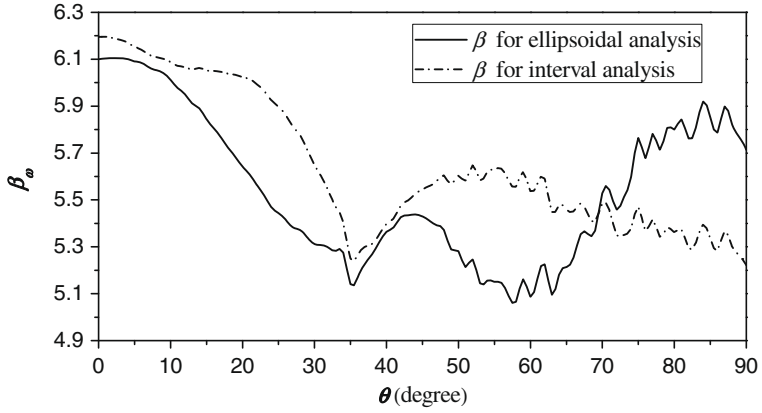

Fig. 5. Degree of uncertainty of the fundamental natural frequency for the 10-layer laminated cylindrical shell.

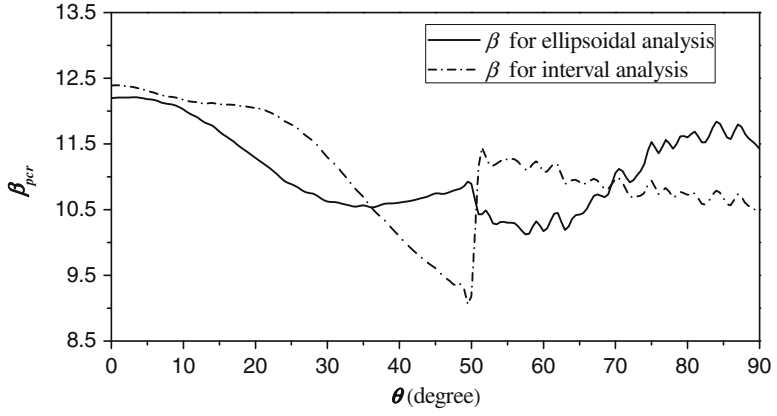

Fig. 6. Degree of uncertainty of the critical external pressure for the 10-layer laminated cylindrical shell.

Acknowledgments

X.W. and Z.Q. thank the National Outstanding Youth Science Foundation of the P.R. China (No. 10425208), 111 Project (No. B07009) and FanZhou Science and Research Foundation for Young Scholars (No. 20080503) for support. I.E. appreciates the financial support by the J.M. Rubin Foundation of the Florida Atlantic University. This study was initiated during I.E.'s stay at Beihang University as a Visiting Professor during April and May 2007. He appreciates the warm and kind hospitality of the International Office (Professor J.X. Ma), faculty (Professor Z.P. Qiu), associates and students.

Appendix. Basic equations for free vibration and buckling of composite shell

Donnell shell theory is used to analysis the buckling of cylindrical shells of composite materials. The strain–displacement relations are

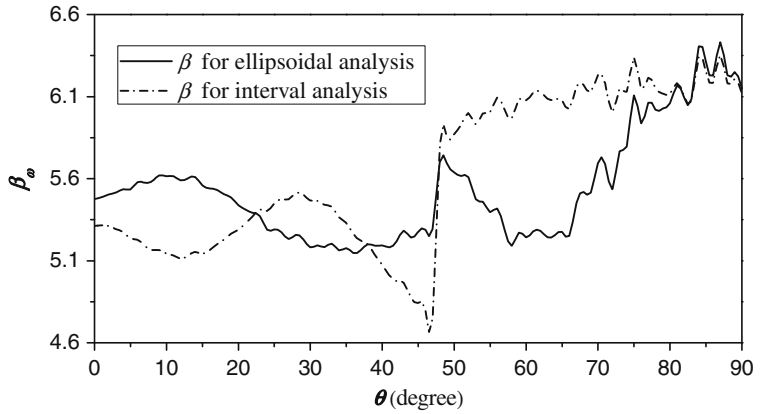

Fig. 7. Degree of uncertainty of the fundamental natural frequency for the 5-layer laminated cylindrical shell.

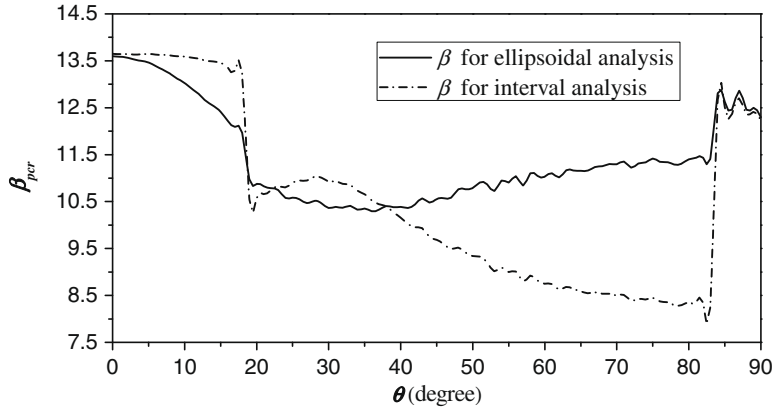

Fig. 8. Degree of uncertainty of the critical external pressure for the 5-layer laminated cylindrical shell.

$$\varepsilon_x = \frac{\partial u}{\partial x}, \quad \varepsilon_y = \frac{\partial v}{\partial y} + \frac{w}{R}, \quad \gamma_{xy} = \frac{\partial v}{\partial x} + \frac{\partial u}{\partial y}$$
$$\kappa_x = -\frac{\partial^2 w}{\partial x^2}, \quad \kappa_y = -\frac{\partial^2 w}{\partial y^2}, \quad \kappa_{xy} = -2\frac{\partial^2 w}{\partial x \partial y} \tag{A.1}$$

where x and y are the axial and circumferential coordinates in the shell middle surface; u and v are the shell displacement along axial and circumferential directions, and w is the radial displacement, positive outward; ε_x, ε_y and γ_{xy} are strain components; κ_x, κ_y and κ_{xy} are middle surface curvature of the shell; R is the radius of the cylindrical shell.

The constitutive relations for the composite laminate read

$$\begin{pmatrix} N_x \\ N_y \\ N_{xy} \\ M_x \\ M_y \\ M_{xy} \end{pmatrix} = \begin{pmatrix} A_{11} & A_{12} & A_{16} & B_{11} & B_{12} & B_{16} \\ A_{12} & A_{22} & A_{26} & B_{11} & B_{22} & B_{26} \\ A_{16} & A_{26} & A_{66} & B_{16} & B_{26} & B_{66} \\ C_{11} & C_{12} & C_{16} & D_{11} & D_{12} & D_{16} \\ C_{12} & C_{22} & C_{26} & D_{12} & D_{22} & D_{26} \\ C_{16} & C_{26} & C_{66} & D_{16} & D_{26} & D_{66} \end{pmatrix} \begin{pmatrix} \varepsilon_x \\ \varepsilon_y \\ \varepsilon_{xy} \\ \kappa_x \\ \kappa_y \\ \kappa_{xy} \end{pmatrix} \tag{A.2}$$

where N_x, N_y and N_{xy} are stress resultants, M_x, M_y and M_{xy} are bending and twisting moments, acting on a laminate; the laminate stiffness A_{ij}, B_{ij} and D_{ij} are defined as

$$(A_{ij}, B_{ij}, D_{ij}) = \int_{-h/2}^{h/2} \overline{Q}_{ij}^{(k)}(1, z, z^2)dz \tag{A.3}$$

where h is the total thickness of the laminate, and z is the coordinate in the direction of the laminate thickness; $\overline{Q}_{ij}$ are the transformed reduced stiffness and can be expressed in terms of the lamina orientation and four independent engineering material constants in principal material directions, i.e., E_1, E_2, ν_{21} and G_{12}.

The equilibrium equations of the cylindrical shell read

$$\begin{aligned} &\frac{\partial N_x}{\partial x} + \frac{\partial N_{xy}}{\partial y} = 0 \\ &\frac{\partial N_{xy}}{\partial x} + \frac{\partial N_y}{\partial y} = 0 \\ &\frac{\partial^2 M_x}{\partial x^2} + 2\frac{\partial^2 M_{xy}}{\partial x \partial y} + \frac{\partial^2 M_y}{\partial y^2} - \frac{1}{R}N_y + N_x\frac{\partial^2 w}{\partial x^2} \\ &\quad + 2N_{xy}\frac{\partial^2 w}{\partial x \partial y} + N_y\frac{\partial^2 w}{\partial y^2} - \rho\frac{\partial^2 w}{\partial t^2} = 0 \end{aligned} \tag{A.4}$$

where ρ is the mass per unit volume of the shell and t is time.

Using Eqs. (A.1) and (A.2), Eq. (A.4) can be written as

$$\begin{pmatrix} L_{11} & L_{12} & L_{13} \\ L_{21} & L_{22} & L_{23} \\ L_{31} & L_{32} & L_{33} \end{pmatrix} \begin{pmatrix} u \\ v \\ w \end{pmatrix} = \begin{pmatrix} 0 \\ 0 \\ N_x\frac{\partial^2 w}{\partial x^2} + 2N_{xy}\frac{\partial^2 w}{\partial x \partial y} + N_y\frac{\partial^2 w}{\partial y^2} - \rho\frac{\partial^2 w}{\partial t^2} \end{pmatrix} \tag{A.5}$$

where the operators L_{ij} are

$$
\begin{aligned}
L_{11} &= A_{11}\frac{\partial^2}{\partial x^2} + 2A_{16}\frac{\partial^2}{\partial x\partial y} + A_{66}\frac{\partial^2}{\partial y^2}\\
L_{12} &= A_{16}\frac{\partial^2}{\partial x^2} + (A_{12}+A_{16})\frac{\partial^2}{\partial x\partial y} + A_{26}\frac{\partial^2}{\partial y^2}\\
L_{13} &= \frac{1}{R}\left(A_{12}\frac{\partial}{\partial x} + A_{26}\frac{\partial}{\partial y}\right) - B_{11}\frac{\partial^2}{\partial x^2} - 3B_{16}\frac{\partial^3}{\partial x^2\partial y}\\
&\quad - (B_{12}+B_{66})\frac{\partial^3}{\partial x\partial y^2} - B_{26}\frac{\partial^3}{\partial y^3}\\
L_{22} &= A_{66}\frac{\partial^2}{\partial x^2} + 2A_{26}\frac{\partial^2}{\partial x\partial y} + A_{22}\frac{\partial^2}{\partial y^2}\\
L_{23} &= \frac{1}{R}\left(A_{26}\frac{\partial}{\partial x} + A_{22}\frac{\partial}{\partial y}\right) - B_{22}\frac{\partial^3}{\partial y^3} - 3B_{26}\frac{\partial^3}{\partial x\partial y^2}\\
&\quad - (B_{12}+2B_{66})\frac{\partial^3}{\partial x^2\partial y} - B_{16}\frac{\partial^3}{\partial x^3}\\
L_{33} &= -\frac{2}{R}\left(B_{12}\frac{\partial^2}{\partial x^2} + 2B_{26}\frac{\partial^2}{\partial x\partial y} + B_{22}\frac{\partial^2}{\partial y^2}\right) + \frac{A_{22}}{R} + D_{11}\frac{\partial^4}{\partial x^4}\\
&\quad + 4D_{16}\frac{\partial^4}{\partial x^3\partial y} + 2(D_{12}+2D_{66})\frac{\partial^4}{\partial x^2\partial y^2} + 4D_{26}\frac{\partial^4}{\partial x\partial y^3} + D_{22}\frac{\partial^4}{\partial y^4}
\end{aligned}
\tag{A.6}
$$

We consider the cylindrical shell with simply supported boundary conditions which are satisfied by the following displacement functions

$$
\begin{pmatrix} u\\ v\\ w \end{pmatrix} = \sum_{m=1}^{\infty}\sum_{n=0}^{\infty}\begin{pmatrix} U_{mn}\cos(\lambda_m x)\cos(\lambda_n y)e^{i\omega t}\\ V_{mn}\sin(\lambda_m x)\sin(\lambda_n y)e^{i\omega t}\\ W_{mn}\sin(\lambda_m x)\cos(\lambda_n y)e^{i\omega t}\end{pmatrix} \tag{A.7}
$$

where $\lambda_m = m\pi/L$, $\lambda_n = n/R$ and ω is the natural frequency of the shell.

Similar to studies by Tasi (1966), and Hirano (1979), here the coupling stiffness $(A_{16}, A_{26}, B_{16}, B_{26}, D_{16}, D_{26})$ are neglected. They actually vanish for symmetric cross-ply laminates. As for symmetric angle-ply laminates, B_{16} and B_{26} are zero, and A_{16}, A_{26}, D_{16} and D_{26} can be neglected for laminates with many layers.

Substitution of Eqs. (A.1) and (A.2) into Eq. (A.4) leads to a set of homogeneous linear algebraic equations, and the existence of non-trivial solutions requires that the determinant of the coefficient matrix vanish

$$
\det\begin{pmatrix} C_{11} & C_{12} & C_{13}\\ C_{21} & C_{22} & C_{23}\\ C_{31} & C_{32} & C_{33} - \lambda_m^2 N_x - \lambda_m\lambda_n N_{xy} - \lambda_n^2 N_y + \rho\omega^2\end{pmatrix} = 0 \tag{A.8}
$$

where elements C_{ij}'s are expressed as

$$
\begin{aligned}
C_{11} &= A_{11}\lambda_m^2 + A_{66}\lambda_n^2\\
C_{22} &= A_{22}\lambda_n^2 + A_{66}\lambda_m^2\\
C_{33} &= D_{11}\lambda_m^4 + 2(D_{12}+2D_{66})\lambda_m^2\lambda_n^2 + D_{22}\lambda_n^4\\
&\quad + \frac{A_{22}}{R} + 2\frac{B_{22}}{R}\lambda_n^2 + 2\frac{B_{12}}{R}\lambda_m^2\\
C_{12} &= C_{21} = (A_{12}+A_{66})\lambda_m\lambda_n\\
C_{23} &= C_{32} = (B_{12}+2B_{66})\lambda_m^2\lambda_n + \frac{A_{22}}{R}\lambda_n + B_{22}\lambda_n^3\\
C_{13} &= C_{31} = \frac{A_{12}}{R}\lambda_m + B_{11}\lambda_m^3 + (B_{12}+2B_{66})\lambda_m\lambda_n^2
\end{aligned}
\tag{A.9}
$$

From Eq. (A.8), the following expression can be readily derived for the natural frequency

$$
\begin{aligned}
\rho\omega^2 &= C_{33} + \frac{(2C_{12}C_{23} - C_{13}C_{22})C_{13} - C_{23}^2 C_{11}}{C_{11}C_{22} - C_{12}^2}\\
&\quad + \lambda_m^2 N_x + \lambda_m\lambda_n N_{xy} + \lambda_n^2 N_y \equiv \rho\omega_{mn,N}^2
\end{aligned}
\tag{A.10}
$$

where the subscript "N" indicates the presence of external loading acting in the mid-surface of the shell.

If the shell in question is free from external loading, i.e., $N_x = N_y = N_{xy} = 0$, the natural frequency becomes

$$
\omega_{mn,0}^2 = \frac{1}{\rho}\left[C_{33} + \frac{(2C_{12}C_{23} - C_{13}C_{22})C_{13} - C_{23}^2 C_{11}}{C_{11}C_{22} - C_{12}^2}\right] \tag{A.11}
$$

where the subscript zero indicates that the external loads acting in the mid-surface of the shell are absent. To determine the fundamental natural frequency for a cylindrical shell with given dimensions and material properties, one determines those integer values of m and n which minimize ω_{mn}. With $\omega = 0$, Eq. (A.10) yields an expression for the buckling load. Consider the buckling of shells under external pressure p, for which

$$
N_y = -pR, \quad N_x = -\frac{pR}{2}, \quad N_{xy} = 0 \tag{A.12}
$$

The expression for the critical external pressure can be readily derived as follows:

$$
p = \frac{2}{(\lambda_m^2 + 2\lambda_n^2)R}\left[C_{33} + \frac{(2C_{12}C_{23} - C_{13}C_{22})C_{13} - C_{23}^2 C_{11}}{C_{11}C_{22} - C_{12}^2}\right] \equiv p_{mn} \tag{A.13}
$$

Again, one has to perform a search with respect to integer variables m and n to minimize the objective function p_{mn} in order to obtain the critical external pressure p_{cr} for a cylindrical shell with given dimensions and material properties.

References

Alefeld, G., Herzberger, J., 1983. Introduction to Interval Computations. Academic Press, New York.

Ben-Haim, Y., Elishakoff, I., 1990. Convex Models of Uncertainty in Applied Mechanics. Elsevier Science Publishers, Amsterdam.

Chernousko, F.L., 1993. State Estimation of Dynamical Systems. CRS Press, Boca Raton.

Elishakoff, I., Li, Y.W., et al., 2001. Non-Classical Problems in the Theory of Elastic Stability. Cambridge University Press, Cambridge.

Goggin, P.R., 1973. The elastic constants of carbon-fibre composites. Journal of Materials Sciences 8, 233–244.

Hansen, E., 1992. Global Optimization Using Interval Analysis. Maecel Dekker Inc., New York.

Hirano, Y., 1979. Buckling of angle-ply laminated circular cylindrical shells. Journal of Applied Mechanics 46, 233–234.

Li, Y.W., Elishakoff, I., et al., 1996. Prediction of natural frequency of buckling load variability due to uncertainty in material properties by convex modeling. Fields Institute Communications 9, 139–154.

Moore, R.E., 1979. Methods and Applications of Interval Analysis. Prentice-Hall, Inc., London.

Neumaier, A., 1990. Interval Methods for Systems of Equations. Cambridge University Press, Cambridge.

Pantelides, C.P., 1996. Buckling and postbuckling of stiffened elements with uncertainty. Thin-walled Structures 26 (1), 1–17.

Qiu, Z.P., 2003. Comparison of static response of structures using convex models and interval analysis method. International Journal for Numerical Methods in Engineering 56 (12), 1735–1753.

Qiu, Z.P., 2005a. Convex Method Based on Non-Probabilistic Set-Theory and its Applications. National Defence Industry Press, Beijing.

Qiu, Z.P., 2005b. Convex models and interval analysis method to predict the effect of uncertain-but-bounded parameters on the buckling of composite structures. Computer Methods in Applied Mechanics and Engineering 194, 2175–2189.

Ramu, S.A., Ganesan, R., 1993. Parametric stability of stochastic columns. International Journal of Solids and Structures 30, 1339–1354.

Tasi, J., 1966. Effect of heterogeneity on the stability of composite cylindrical shells under axial compression. AIAA Journal 4, 1059–1062.

Tewary, V.K., 1978. Mechanics of Fiber Composites. Wiley, New York.

Wang, X.J., Elishakoff, I., et al., 2008. Experimental data have to decide which of the non-probabilistic uncertainty descriptions – convex modeling or interval analysis – to utilize. Journal of Applied Mechanics 75 (4), 1–8.

Zhu, L.P., Elishakoff, I., et al., 1996. Derivation of multi-dimensional ellipsoidal convex model for experimental data. Mathematical and Computer Modelling 24 (2), 103–114.